# Transport theory in non-Hermitian systems

Qing Yan[1], Hailong Li[1], Qing-Feng Sun[1,2,*] and X. C. Xie[1,2,3,†]

[1]*International Center for Quantum Materials, School of Physics, Peking University, Beijing 100871, China*

[2]*Hefei National Laboratory, Hefei 230088, China*

[3]*Interdisciplinary Center for Theoretical Physics and Information Sciences (ICTPIS), Fudan University, Shanghai 200433, China*

(Received 26 July 2022; revised 30 June 2024; accepted 3 July 2024; published 19 July 2024)

Non-Hermitian systems have garnered significant attention due to the emergence of novel topology of complex spectra and skin modes. However, investigating transport phenomena in such systems faces obstacles stemming from the nonunitary nature of time evolution. Here, we establish the continuity equation for a general non-Hermitian Hamiltonian in the Schrödinger picture. It attributes the universal nonconservativity to the anti-commutation relationship between particle number and non-Hermitian terms. Our paper derives a comprehensive current formula for non-Hermitian systems using Green's function, applicable to both time-dependent and steady-state responses. To demonstrate the validity of our approach, we calculate the local current of models with one-dimensional and two-dimensional settings, incorporating scattering potentials. The spatial distribution of local current highlights the widespread non-Hermitian phenomena, including skin modes, nonreciprocal quantum dots, and corner states. Additionally, we revisit a recent experiment within the quantum Hall regime and propose a set-up for experimentally detecting non-Hermitian current. Our findings offer valuable insights for advancing theoretical and experimental research in the transport of non-Hermitian systems.

DOI: 10.1103/PhysRevB.110.045138

## I. INTRODUCTION

Current in physical systems is a response to the external excitation. Being accurately measured in transport experiments, the current-voltage characteristic and current fluctuations faithfully reflect intrinsic physical properties both statically and dynamically [1–5]. Notably, in recently reported topological systems, such as the quantum Hall insulator or the quantum anomalous Hall insulator [6–8], a precisely quantized current signature shows the robust edge mode protected by the topology of bands [9,10]. In these Hermitian quantum systems, the unitary nature of the time-evolution operator ensures the conservation of both the particle number $n$ and current $\boldsymbol{j}$, i.e., the continuity equation $\frac{\partial n}{\partial t} + \nabla \cdot \boldsymbol{j} = 0$ [11,12].

Non-Hermitian systems are in hot spots for their exotic properties [13–16], including non-Hermitian topology, unusual bulk-edge correspondence, skin modes and possible unidirectional amplification [17–31]. For non-Hermitian open chains, skin modes manifest as bulk eigenstates localized at boundaries, exhibiting exponential-decay behavior [25]. Recent progress has focused on the properties of eigenstates, which have been observed in both classical and quantum systems including optics and photonics, topoelectrical circuits, metamaterials, cold atom systems, and quantum walk systems [32–39]. Beyond their stationary properties, transport techniques can reveal the dynamical response of bulk eigenmodes in non-Hermitian systems. However, exploring the transport properties of these systems remains challenging due to the nonunitary nature of the time-evolution operator [40]. This nonunitarity further leads to a significant issue during time evolution: The traditional continuity equation requires reevaluation. Given these intricacies, it is crucial to establish the transport theory for non-Hermitian systems.

Addressing the challenges outlined, we investigate the continuity equation for non-Hermitian systems based on the Schrödinger picture. We introduce a modified continuity equation, applicable to non-Hermitian Hamiltonians, which incorporates a critical anticommutation term. The anticommutator indicates a clear distinction from Hermitian systems and directly leads to the phenomenon of nonconservation in non-Hermitian scenarios, affecting physical quantities such as particle number and local current. Employing Green's function approach, we derive a generalized current formula that captures both temporal and steady-state responses of non-Hermitian systems. Applied to one-dimensional (1D) and two-dimensional (2D) non-Hermitian Hatano-Nelson (HN) models, particularly under the effect of scattering potentials, the current formula reveals the unique features of skin modes, nonreciprocal quantum dots, and corner states. Besides, we reexamine a recent experiment in the quantum Hall (QH) regime and propose the experimental detection of the non-Hermitian current. Our findings pave the way for further exploration into the dynamic behaviors of non-Hermitian systems.

The paper is organized as follows. Section II begins by deriving the general form of the continuity equation for non-Hermitian systems, highlighting its distinct characteristics compared to Hermitian systems. Following this, the explicit formula of local current in terms of Green's function is derived in Sec. III, including the time-dependent current and stead-state current in both the continuous and discrete form.

*Contact author: sunqf@pku.edu.cn

†Contact author: xcxie@pku.edu.cn

 

Subsequent sections, Secs. IV to VI, illustrate specific examples of local current calculations. These range from the analytical expressions of 1D HN model (Sec. IV), the numerical transport result through a scattering potential in 1D case (Sec. V), and extending to the 2D HN model (Sec. VI). An experimental proposal related to these findings is discussed in Sec. VII. The paper concludes with a summary and future outlook in Sec. VIII.

## II. CONTINUITY EQUATION

For any non-Hermitian system, the Hamiltonian can always be decomposed into Hermitian and anti-Hermitian parts, denoted as $\hat{H} = \hat{H}_{\mathrm{H}} + \hat{H}_{\mathrm{A}}$, where $\hat{H}^\dagger = \hat{H}_{\mathrm{H}} - \hat{H}_{\mathrm{A}}$. Given a state $|\Phi(t)\rangle$ and the particle number density operator defined as $\hat{n}(\boldsymbol{r}) = \hat{\psi}^\dagger(\boldsymbol{r})\hat{\psi}(\boldsymbol{r})$, its expectation value at time $t$ is given by $\langle \hat{n}(\boldsymbol{r})\rangle_t := \langle \Phi(t)|\hat{n}(\boldsymbol{r})|\Phi(t)\rangle$ [39,41,42]. Although the density of particle number $n$ may not be conservative, it still serves as a physical observable in non-Hermitian systems, which can be measured in experiments, such as the dissipative cold atom system in Ref. [38] or the single-photon quantum walk system with loss terms in Ref. [39]. Provided that the state evolves according to the Schrödinger equation, $i\frac{\partial}{\partial t}|\Phi(t)\rangle = \hat{H}|\Phi(t)\rangle$, the time evolution of the particle number density is expressed as

$$\frac{\partial}{\partial t}\langle \hat{n}(\boldsymbol{r})\rangle_t = \frac{1}{i\hbar}\langle[\hat{n}(\boldsymbol{r}), \hat{H}_{\mathrm{H}}]\rangle_t + \frac{1}{i\hbar}\langle\{\hat{n}(\boldsymbol{r}), \hat{H}_{\mathrm{A}}\}\rangle_t, \tag{1}$$

This represents the general form of the continuity equation in the second quantization form in the Schrödinger picture. The terms on the right-hand side of Eq. (1) correspond to the commutator/anticommutator between $\hat{n}(\boldsymbol{r})$ and the Hermitian/anti-Hermitian parts of the Hamiltonian, $\hat{H}_{\mathrm{H}}/\hat{H}_{\mathrm{A}}$, respectively.

In the Hermitian case, the local current operator $\hat{\boldsymbol{j}}(\boldsymbol{r})$ can be derived straightforwardly from the time derivative of $\hat{n}(\boldsymbol{r})$ in the Heisenberg picture, even when interaction terms are present [43–45]. However, this approach is not applicable to non-Hermitian Hamiltonians due to the absence of a closed and unitary time-evolved operator. Therefore, we employ the Schrödinger picture when deriving the general continuity equation.

We consider the Hamiltonian in the form of $\hat{H} = \hat{H}_0 + \hat{H}_{\mathrm{int}} + \hat{H}_{\mathrm{A}}$ where the Hermitian part is divided into noninteracting ($\hat{H}_0$) and interacting ($\hat{H}_{\mathrm{int}}$) parts. Let $\hat{H}_0 = \int d\boldsymbol{r}\ \ \hat{\psi}^\dagger(\boldsymbol{r})(a\hat{\boldsymbol{p}}^2 + \hat{V}(\boldsymbol{r}))\hat{\psi}(\boldsymbol{r})$ represent the noninteracting part. For the anti-Hermitian part, two common non-Hermitian ingredients are considered, $\hat{H}_{\mathrm{A}} = \int d\boldsymbol{r}\ \ \hat{\psi}^\dagger(\boldsymbol{r})(i\boldsymbol{\beta}\cdot\hat{\boldsymbol{p}} + i\gamma)\hat{\psi}(\boldsymbol{r})$. By inserting $\hat{H}$ into Eq. (1), the continuity equation becomes

$$\frac{\partial}{\partial t}\langle \hat{n}(\boldsymbol{r})\rangle_t + \nabla\cdot\langle\hat{\boldsymbol{j}}(\boldsymbol{r})\rangle_t = \frac{2\gamma}{\hbar}\langle \hat{n}(\boldsymbol{r})\rangle_t + \frac{\boldsymbol{\beta}}{a}\cdot\langle\hat{\boldsymbol{j}}(\boldsymbol{r})\rangle_t, \tag{2}$$

where the local current operator is directly obtained from the first term of $[\hat{n}(\boldsymbol{r}), \hat{H}_0]$ in Eq. (1),

$$\hat{\boldsymbol{j}}(\boldsymbol{r}) = \frac{a}{i\hbar}(\hat{\psi}^\dagger(\boldsymbol{r})\nabla\hat{\psi}(\boldsymbol{r}) - (\nabla\hat{\psi}^\dagger(\boldsymbol{r}))\hat{\psi}(\boldsymbol{r})). \tag{3}$$

Remarkably, both non-Hermitian $\beta$ and $\gamma$ impact and modify the continuity equation Eq. (2), ultimately leading to exotic non-Hermitian phenomena. Unlike non-Hermitian spectra or eigenstates, which are sensitive to boundary conditions, it is essential to emphasize that the continuity equation remains robust regardless of boundary conditions (refer to Appendix A).

The continuity equation (2) can accommodate interacting terms, such as the Coulomb interaction $\hat{H}_{\mathrm{int}} = \frac{1}{2}\int d\boldsymbol{r}d\boldsymbol{r}' v(\boldsymbol{r},\boldsymbol{r}')\hat{\psi}^\dagger(\boldsymbol{r})\hat{\psi}^\dagger(\boldsymbol{r}')\hat{\psi}(\boldsymbol{r}')\hat{\psi}(\boldsymbol{r})$. Since the commutator $[\hat{n}(\boldsymbol{r}), \hat{H}_{\mathrm{int}}]$ vanishes, these interactions maintain both the form of the continuity equation and the definition of the local current even in the presence of a nonzero $H_A$. When the non-Hermitian terms are absent, the continuity equation in Eq. (2) reduces to its Hermitian form, $\frac{\partial}{\partial t}\langle \hat{n}(\boldsymbol{r})\rangle_t + \nabla\cdot\langle\hat{\boldsymbol{j}}(\boldsymbol{r})\rangle_t = 0$.

The unique manner of nonconservation of current as indicated by Eq. (1) is specific to non-Hermitian systems. While the nonconservative current also exists in Hermitian systems, its underlying cause significantly differs from the scenario presented here. In a Hermitian system, the nonconservation term arises from the nonzero commutator between the particle number operator and the Hamiltonian; for instance, the nonconservative phonons current [46,47]. But for non-Hermitian systems, the correct form of the continuity equation requires the incorporation of anticommutation relationships, like the two terms on right-hand side of Eq. (2) under consideration. Our approach specifically targets the unique correction protocol for the continuity equation when non-Hermitian terms are present, which distinguishes it from the established Hermitian paradigm. Up to this point, the phenomena of nonconservation in both Hermitian and non-Hermitian systems have been integrated into a unified framework, as presented in Eq. (1).

## III. NON-HERMITIAN CURRENT FORMULAS VIA GREEN'S FUNCTION: TIME-DEPENDENT AND STEADY-STATE

Green's function is an extremely powerful technique in transport theory, especially for calculating the time-dependent and steady-state current regardless of the system's geometric shape and even in the presence of interactions [43–45,48,49]. For non-Hermitian mesoscopic systems, we are to derive a general current formula expressed by Green's function in both the continuous and discrete forms.

### A. Time-dependent current formula

For an arbitrary wavefunction $|\Phi(t)\rangle$, the local current $\langle\hat{\boldsymbol{j}}\rangle_t$ is calculated as the expectation value of the operator derived from Eq. (1). Subsequently, we turn to the transport phenomena where the wave function $|\Phi(t)\rangle$ is evolved from an injected state, $|\Phi_0(t')\rangle$ at time $t'$. Given an arbitrary Hamiltonian $H = H_0 + H_{\mathrm{A}} + H_{\mathrm{int}}$, the time-dependent Green's function is defined as [50]

$$\left(i\frac{\partial}{\partial t} - H\right)G(\boldsymbol{r},\boldsymbol{r}';t,t') = \delta(\boldsymbol{r}-\boldsymbol{r}')\delta(t-t'), \tag{4}$$

where $G(\boldsymbol{r},\boldsymbol{r}';t,t')$ is the Green's function of the Schrödinger equation, $(i\frac{\partial}{\partial t} - H)\Phi(\boldsymbol{r},t) = 0$. Whether the Hamiltonian $H$

is time dependent, one can solve the corresponding $G$ and obtain the evolved state, $|\Phi(t)\rangle = i[\hat{G}^r(t,t') - \hat{G}^a(t,t')]|\Phi_0(t')\rangle$ with $G^{r/a}(\boldsymbol{r},\boldsymbol{r}';t,t') = \langle\boldsymbol{r}|\hat{G}^{r/a}(t,t')|\boldsymbol{r}'\rangle$. The subscripts $r/a$ denotes the retarded/advanced function, $G^{r/a}$, respectively. Then, substitute it into Eq. (3) and compute the local current $\boldsymbol{j}$ at $(\boldsymbol{r},t)$, which is decomposed as $\boldsymbol{j}(\boldsymbol{r},t) = \sum_{\mu=1}^{d} j_\mu \boldsymbol{e}_\mu$ with $d$ the dimensionality of the system and $\boldsymbol{e}_\mu$ being the unit vector in real space. The temporal local current is

$$j_\mu(\boldsymbol{r};t) = -\frac{2a}{\hbar}\int d\boldsymbol{r}'d\boldsymbol{r}''\mathrm{Im}[G^r(\boldsymbol{r},\boldsymbol{r}'';t,t')\Phi_0(\boldsymbol{r}'',t') \times \frac{\partial}{\partial \boldsymbol{r}_\mu}(\Phi_0^*(\boldsymbol{r}',t')G^a(\boldsymbol{r}',\boldsymbol{r};t',t))]. \quad (5)$$

This formula represents a main result of this paper. It offers an exact expression for the local current in terms of Green's functions of the non-Hermitian regime. It remains valid in the presence of various interactions, scattering potentials or random disorder.

### B. Steady-state current formula

We further consider the steady-state transport when the Hamiltonian $H$ is time independent. We consider a constant injection state $|\Phi_0(t')\rangle \equiv |\Phi_0\rangle$ at any time $t'$ before the observing time $t$. For any time $t'$, there is a response current at time $t$, $j_\mu(\boldsymbol{r};t,t')$ as in Eq. (5). Thus, the local current at $t$ is the sum of all the response with the injection time before $t$, expressed as $I_\mu(\boldsymbol{r}) = \int_{-\infty}^{t} dt' j_\mu(\boldsymbol{r};t,t')$.

Within a steady state, local current in Eq. (5) together with Green's functions in Eq. (4) depend only on the time difference $t-t'$ and thus can be Fourier transformed into energy domain, yielding $I_\mu(\boldsymbol{r}) = \int_{-\infty}^{+\infty} d\epsilon\ \ j_\mu(\boldsymbol{r},\epsilon)$ (refer to Appendix B). Therefore, for an injection state characterized by certain energy $\epsilon$, the steady-state local current along the $\mu$-direction at position $\boldsymbol{r}$ is

$$j_\mu(\boldsymbol{r},\epsilon) = \frac{-a}{\pi\hbar}\int d\boldsymbol{r}'d\boldsymbol{r}''\mathrm{Im}\Big[G^r(\boldsymbol{r},\boldsymbol{r}'';\epsilon)\Phi_0(\boldsymbol{r}'') \times \Phi_0^*(\boldsymbol{r}')\frac{\partial}{\partial \boldsymbol{r}_\mu}G^a(\boldsymbol{r}',\boldsymbol{r};\epsilon)\Big]. \quad (6)$$

Here, we discuss the steady-state condition of Eq. (6). In a Hermitian system, if the Hamiltonian is time independent, it can always reach a steady state wherein energy and current are conserved [43]. However, for non-Hermitian systems, a time-independent Hamiltonian hardly guarantees a steady state, as the presence of nonzero imaginary parts in the energy spectrum obviously disrupts the particle number conservation. We reveal that achieving a steady state requires that energy spectra possess nonpositive imaginary parts; otherwise, achieving a steady state might not be possible. Consequently, the derived steady-state current in Eq. (6) is applicable to non-Hermitian systems with energy spectra possessing nonpositive imaginary components.

In transport research, the continuous model provides theoretical foundations, while the discrete model offers greater numerical flexibility in modeling realistic non-Hermitian systems. Building on this, we derive the discrete form of the steady-state local current in Eq. (6) (for details refer to Appendix B),

$$j\left(\boldsymbol{R}+\frac{1}{2}\boldsymbol{a}_\mu,\epsilon\right) = \frac{-a}{\pi\hbar a_0}\sum_{\boldsymbol{R}',\boldsymbol{R}''}\mathrm{Im}\Big[G^r_{\boldsymbol{R},\boldsymbol{R}''}(\epsilon)\Phi_0(\boldsymbol{R}'') \times \Phi_0^*(\boldsymbol{R}')G^a_{\boldsymbol{R}',\boldsymbol{R}+\boldsymbol{a}_\mu}(\epsilon)\Big]. \quad (7)$$

Equation (7) represents the local current from site $\boldsymbol{R}$ to its neighboring site $\boldsymbol{R}+\boldsymbol{a}_\mu$. Here $a_0$ is the discretized lattice constant and $\boldsymbol{a}_\mu$ is the unit lattice vector in the $\mu$ direction.

Further, for a pulse-like injection in position space, $|\Phi_0(\boldsymbol{R})|^2 = |A|^2/a_0\ \delta_{\boldsymbol{R},\boldsymbol{R}_0}$, at certain position $\boldsymbol{R}_0$ with amplitude $A$, Eq. (7) can be simplified as

$$j\left(\boldsymbol{R}+\frac{1}{2}\boldsymbol{a}_\mu,\epsilon\right) = \frac{2}{h}t^{\mathrm{H}}_{\boldsymbol{R},\boldsymbol{R}+\boldsymbol{a}_\mu}|A|^2\mathrm{Im}\Big[G^r_{\boldsymbol{R},\boldsymbol{R}_0}(\epsilon)G^a_{\boldsymbol{R}_0,\boldsymbol{R}+\boldsymbol{a}_\mu}(\epsilon)\Big], \quad (8)$$

with $t^{\mathrm{H}}_{\boldsymbol{R},\boldsymbol{R}+\boldsymbol{a}_\mu} = -a/a_0^2$. The coefficient $t^{\mathrm{H}}_{\boldsymbol{R},\boldsymbol{R}+\boldsymbol{a}_\mu}$ picks the hopping term between neighboring sites in the Hermitian part, $H_0$. The non-Hermitian features of the system are captured in Green's functions, as derived from Eq. (4), which lead to the emergence of nonconservation in the local current. When $H$ is Hermitian, it reverts to the conventional local current expression [51]. Further, when considering only two terminals, such expression reduces to the two-terminal conductance (refer to Appendix C).

In the following sections, we utilize the derived current formula in Eqs. (6) and (7) to analyze the transport properties of some specific non-Hermitian models.

## IV. ANALYTICAL STEADY-STATE CURRENT OF 1D HN MODEL

The general current formula in Eqs. (6) and (7) is applicable to various non-Hermitian system and the only required ingredients are Green's functions. Here, we take the 1D HN model, which is a prototypical non-Hermitian system, as an example to analytically derive the steady-state local current.

### A. Local current of the continuous 1D HN model

We first discuss the steady-state current of a continuous 1D HN model of which the Hamiltonian is given by [52–54]

$$\hat{H}_{\mathrm{1DHN}} = \int dx\ \hat{\psi}^\dagger(x)\big(a\hat{p}_x^2 + i\beta\hat{p}_x + i\gamma\big)\hat{\psi}(x). \quad (9)$$

Two non-Hermitian terms, $\beta$ and $i\gamma$, correspond to a nonreciprocal hopping term and homogeneous on-site gain/loss term, respectively. When considering the steady-state transport, $\gamma$ is taken to be nonpositive, i.e., Eq. (9) is dubbed as "dissipative HN model". For an infinite HN chain with a continuous injection, $|\Phi_0(x)|^2 = |A|^2\ \delta_{x,x_0}$, at certain position $x_0$ with amplitude $A$, we solve the Green's function in Eq. (4), substitute it into Eq. (6), and thereby the analytical current is

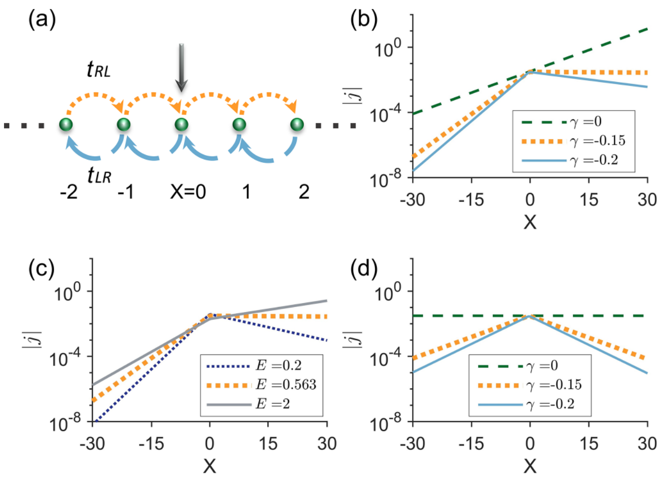


FIG. 1. (a) Schematic diagram of an infinite HN chain. The nearest hopping $t_{\mathrm{LR}}$ and $t_{\mathrm{RL}}$ being discretized from the nonreciprocal term. [(b)–(d)] Steady-state local current $j$ of an infinite HN chain with a continuous injection at position $X = 0$. The dashed line with $\gamma = 0$ in (b) presents the exponentially growing $|j|$ of skin modes. The nonreciprocality in (b) and (c) signifies the existence of skin modes as compared with (d). Parameters are the nonreciprocal term $\beta = 0.2$ for (b) and (c), $\beta = 0$ for (d), the injecting energy $E = 0.563$ in (b) and (d), the on-site loss term $\gamma = -0.15$ in (c).

derived as

$$j(x,\epsilon) = \mp\frac{a}{\pi\hbar}|A|^2\frac{\cos\frac{\varphi}{2}}{4\sqrt{|z_p|}}e^{(\frac{\beta}{a}\pm2\sqrt{|z_p|}\sin\frac{\varphi}{2})(x-x_0)}, \qquad (10)$$

where $z_p = |z_p|e^{i\varphi} = (\epsilon - \beta^2/4 - i\gamma)/a$ assuming $\mathrm{Re}z_p > 0$ and $\mathrm{Im}\sqrt{z_p} > 0$. Here, the upper and lower parts in $\mp(\pm)$ correspond to the cases $x > x_0$ and $x < x_0$. When the injecting energy exceeds the bottom of the energy spectrum, $\epsilon > \beta^2/4$, a finite current is observed in both left ($x < x_0$) and right ($x > x_0$) directions. For $\beta = \gamma = 0$, $j$ remains constant on both sides, thereby adhering to Hermitian current conservation. However, when $\beta$ is nonzero, the current exhibits an exponential growth/decay, $j \propto e^{(\beta/a\pm2\sqrt{|z_p|}\sin\varphi/2)x}$. This spatial variation breaks the current conservation but fulfills the newly derived continuity equation in Eq. (2) (refer to Appendix D).

### B. Local current of the discrete 1D HN model

From the continuous to the discrete model, we consider the 1D HN lattice model with the Hamiltonian being discretized from the continuous model in Eq. (9) as follows:

$$H_{\mathrm{HN}} = \sum_i \epsilon_{\mathrm{on}}c_i^\dagger c_i + t_{\mathrm{LR}}c_i^\dagger c_{i+1} + t_{\mathrm{RL}}c_{i+1}^\dagger c_i. \qquad (11)$$

Here, $\epsilon_{\mathrm{on}} = \frac{2a}{a_0^2} + i\gamma$, $t_{\mathrm{LR}} = -\frac{a}{a_0^2} + \frac{\beta}{2a_0}$, and $t_{\mathrm{RL}} = -\frac{a}{a_0^2} - \frac{\beta}{2a_0}$ with $a_0$ being the lattice constant. Note that for a steady-state response, $\gamma$ is required to be nonpositive.

The local current of the HN lattice model in Fig. 1(a) is also analytically calculated by Eq. (7) with the injection at $x_0 = 0$. Local current in Fig. 1 is analytically calculated by the Green's function based on a discretized lattice Hamiltonian, following the procedure in Appendix E. Other parameters are $a = 1$ and the lattice constant $a_0 = 0.5$. The local current $|j|$ with $\beta > 0$ spatially grows with $\beta$ being the exponential factor in Fig. 1(b) (see the dashed line). Here, the steady-state current with the exponential distribution differs from the constant current of a Hermitian chain in Fig. 1(d), which matches Eq. (10) and also fits the continuity equation. Considering the on-site loss term $\gamma$, the reciprocity of local current distinguishes the non-Hermitian system with/without skin modes, i.e., $|j(-x)| \neq |j(x)|$ in Figs. 1(b) and 1(c) contrasting $|j(-x)| = |j(x)|$ in Fig. 1(d). With moderate loss, the energy-dependent spatial distribution further highlights such nonreciprocality in Fig. 1(b). Away from the injection point, $|j(x < 0)|$ consistently decays, while $|j(x > 0)|$ can be decaying, constant or even growing based on injection energy. Thus, the local current characterizes non-Hermitian transport and identifies skin modes through nonreciprocity.

Compared to the continuous model, the derivation of local current in the discrete model presents more complexities. The core ingredients lie in the analytical expression of Green's function for a lattice model. Therefore, we have provided a detailed derivation framework in the Appendix E, which includes the semi-infinite lattice Green's function, the transfer matrix method, and the analytical expressions for local current within the discrete model. We also showcase the fulfillment of the discrete continuity equation. This derivation, while originating from Hermitian systems, requires additional consideration due to the inherent non-Hermiticity of the systems under study. The methods outlined are applicable across various non-Hermitian lattice models.

## V. SCATTERING BETWEEN A DOUBLE POTENTIAL BARRIER

Beyond the homogenous structure, scattering phenomena hold crucial significance within quantum systems. Functional devices can utilize the double barrier setup to form a quantum dot with discrete energy levels accompanied by the resonant tunneling phenomena [2,3,55]. A symmetrical double barrier is introduced to the 1D non-Hermitian HN model with potential configuration, $V(x) = V_0[\Theta(x - b_1 - L) - \Theta(x - b_1)] + V_0[\Theta(x - b_2 - L) - \Theta(x - b_2)]$, $V_0$ is the height of barriers, $L$ is the length of barriers, and $b_1$ and $b_2$ mark the left positions of the potential barriers. In the calculation of Fig. 2, the length of HN chain is 40. Other Parameters are $b_1 = 17$, $b_2 = 23$, $L = 2$, and $V_0 = 3.5$. Under open boundary conditions, the eigenfunction in Fig. 2(a) showcases characteristic skin modes. Simultaneously, a bundle of isolated bound states emerges within the spatial constraints of the double barrier, notably with their distribution primarily extending towards the right.

For transport measurements, we couple the system to two terminal leads, enabling electron injection with energy $E$ from the left and calculate the steady-state current by Eq. (7). Local current emerges only when the incident energy aligns with the discrete levels of bound states in the quantum dot, consistent with quantum resonant tunneling characteristics [Figs. 2(b) and 2(c)]. Interestingly, unlike its Hermitian counterpart, the local current along the non-Hermitian chain does not remain constant in real space, as evidenced by the different magnitude between $j(X = 10)$ and $j(X = 30)$. This nonconservation is

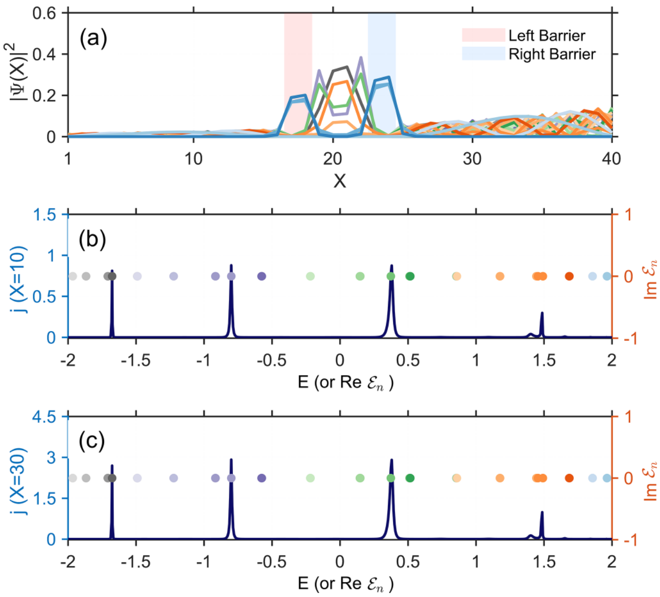


FIG. 2. (a) Distribution of eigenstates $|\Psi(X)|^2$ for a finite HN chain featuring double potential barriers (two shaded regions) reveals an accumulation of skin modes at the right end, while the discrete states formed between the barriers signify nonreciprocal energy levels characteristic of a quantum dot. The corresponding discrete eigenenergies ($\mathrm{Re}\mathcal{E}_n, \mathrm{Im}\mathcal{E}_n$) are plotted as colorful scatters in (b) and (c) in the complex plane–horizontal for real parts and the right vertical axis for imaginary parts. The steady-state local current $j$ versus injecting energy $E$ in (b) and (c) is extracted at sites $X = 10$ and $X = 30$, respectively. The peaks of the local current precisely coincide with the discrete levels of bound states in the quantum dot. Parameters are $t_{\mathrm{RL}} = 1.03$, $t_{\mathrm{LR}} = 0.97$ and $\epsilon_{\mathrm{on}} = 0$.

encoded in the positive nonreciprocal term $\beta$, causing the local current to amplify exponentially from the left injection. Conversely, local current attenuates exponentially from the right injection (refer to Fig. 3). As the length of HN chain approaches its thermodynamic limit, unidirectional conductivity only emerges at these resonant tunneling energies. This behavior highlights the features of the nonreciprocal quantum dot, confined by double barriers along a non-Hermitian chain: not only does it resonate, but it also selectively amplifies or attenuates signals in a unidirectional manner.

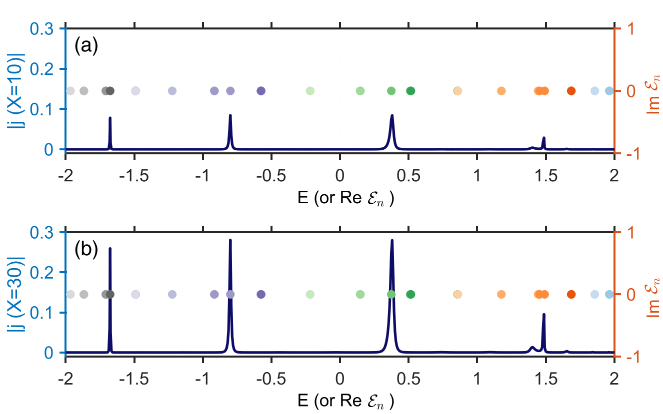


FIG. 3. Local current of a finite-HN chain with double potential barriers where the injection is from the right side. The steady-state local current $j$ vs injecting energy $E$ in (a and b) is extracted at sites $X = 10$ and $X = 30$, respectively. The peaks of the local current precisely coincide with the discrete levels of bound states in the quantum dot, which is the same as the Fig. 2.

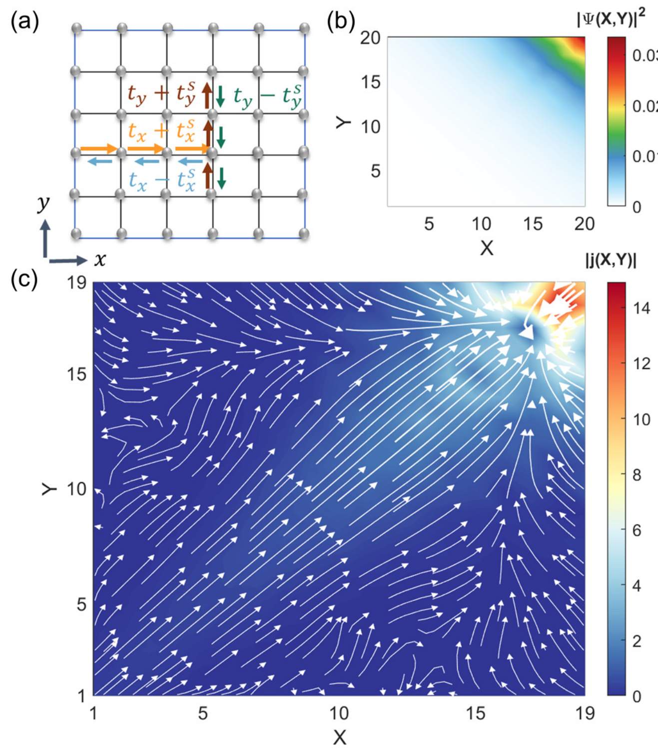


FIG. 4. (a) Schematic diagram of a 2D finite-HN square with nonreciprocal hopping along the $x/y$ direction. (b) Distribution of eigenstates $|\Psi(X, Y)|^2$ of the 2D HN square reveals the corner mode at the top right. (c) A streamline plot depicting the steady-state local current $|j(X, Y)|$ showcases continuous injection from $(X, Y) = (1, 1)$ and at a certain energy $E = 0.12$. The color reflects the absolute value at each site, while arrows with wavy lines denote the corresponding current direction. Parameters are $t_x = t_y = 1$, $t_x^s = t_y^s = 0.1$, and $\gamma = -0.1$.

## VI. TWO-DIMENSIONAL NON-HERMITIAN REGIME

The application of the current formula in Eq. (7) can also extend to 2D systems. In a 2D HN model, nonreciprocal hopping terms are present along both $x$ and $y$ directions, as depicted in Fig. 4(a). To investigate the steady-state distribution of local current within the system, we uniformly introduce a dissipation term of $i\gamma$ to each site on the 2D finite-square lattice. Under open boundary condition (OBC), the eigenstates are localized at the top right [refer to Fig. 4(b)], serving as a hallmark of the non-Hermitian corner-skin effect in high-dimensional systems [56]. Considering the injection of particles with specific energies $E$ from the lower left corner, we proceed to compute the local current of the 2D finite system based on Eq. (7). As illustrated in Fig. 4(c), the local current presents with a pronounced increase in magnitude towards the upper right corner. This observation distinctly

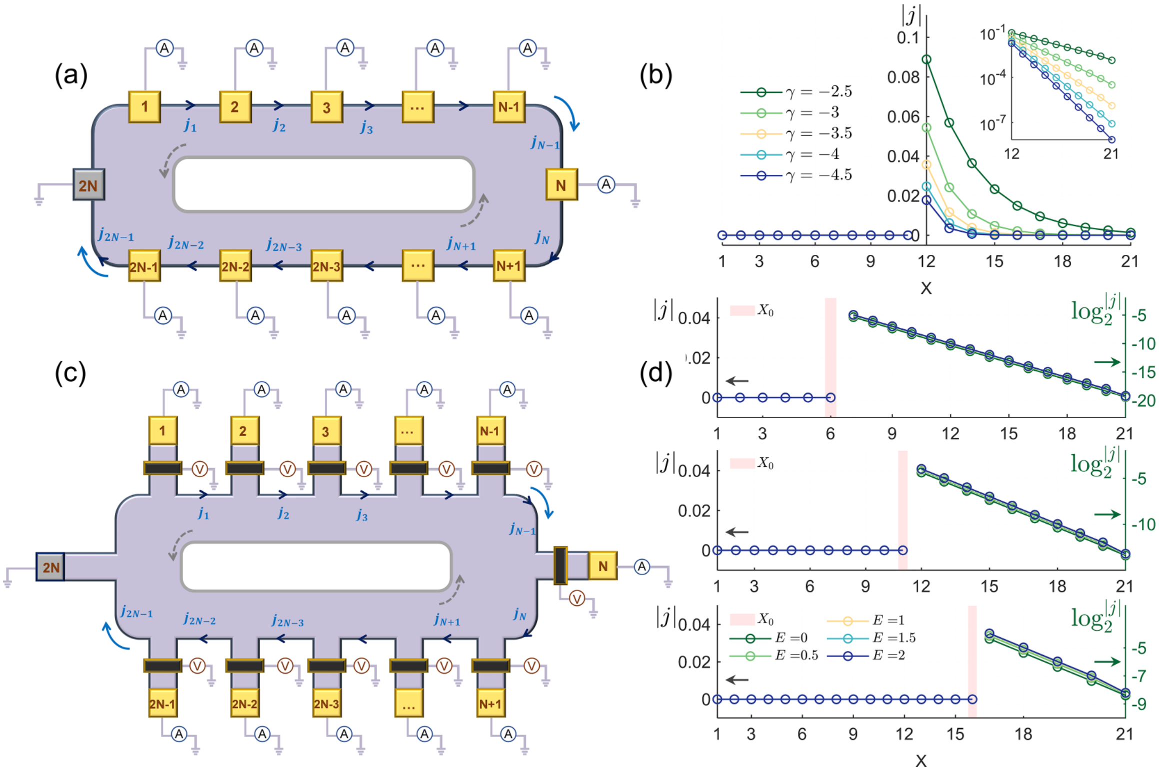

FIG. 5. Experimental detection set-up and non-Hermitian transport. [(a), (c)] Schematic diagram of QH-based HN model with $2N-1$ sites where the contacts connected by chiral edge modes serve as lattice cite with natural nonreciprocal hopping. [(b), (d)] Steady-state local current $|j(X)|$ showcase the continuous injection from $X_0$ and with certain lossy strength $\gamma=-2.5,-3,-3.5,-4,-4.5$ in (b) and with certain injection energy $E=0, 0.5, 1, 1.5, 2$ in (d). $X_0$ picks the value 11 in (b) and values 6, 11, 16 in (d). Local current flowing left/rightward is plotted with a linear/logarithmic axis.

showcases the characteristics of the non-Hermitian corner state.

## VII. EXPERIMENTAL SET-UP FOR DETECTING THE NON-HERMITIAN TRANSPORT

The experimental applicability of our theory can be testified across diverse physical platforms [32–39,57]. In particular, the recent experimental realization of the HN model within the quantum Hall (QH) regime, as reported in Ref. [57], demonstrates non-Hermitian topology through the observation of skin modes with exponential profiles. Despite the pronounced results, such experiment still measures the static properties of the system of which the conductance matrix stimulates a non-Hermitian Hamiltonian, rather than the time evolution of a non-Hermitian Hamiltonian. However, it provides a fantastic platform to actually measure the transport of non-Hermitian signature.

We propose a current measurement set-up based on the QH regime in Fig. 5. By adding $2N$ contacts to a Cobino ring structure, the HN lattice model with extremely nonreciprocal hopping is achieved as in Fig. 5(a). The former $2N-1$ contacts serve as the lattice site, which are connected via chiral edge modes in QH status, i.e., $t_{n,n+1}=2\neq 0$ and $t_{n+1,n}=0$. Here, each contact-$n$ ($n<2N$) is grounding and connects with an ammeter, which further serves as dissipation sources in a reduced non-Hermitian Hamiltonian, $i\gamma$. The last contact label by $2N$ is always grounding, ensuring the OBC of the HN chain. Applying the formula in Eq. (7), the steady-state local current is plotted in Fig. 5(b). At the site right from the injection point ($X_0=11$), i.e., current flowing towards the direction the same as the chirality of QH mode, the local current decays exponentially, as predicted by the analytical formula in Eq. (8) and numerical results in Fig. 1(b). At the left side, the local current always keeps zero since propagation is totally forbidden by the QH chirality. The set-up in Fig. 4(a) is very similar to that in Ref. [57], excepting contacts are set to be grounding instead of floating. In experiments, since each branch of current leaking via contact-$n$ is measurable, the local current can therefore be observed.

We also notice that another set-up is proposed in Ref. [57] of which the results can be exactly reproduced via our non-Hermitian transport theory. The set-up in Fig. 5(c) added additional floating voltage probes within the current probes. Given the chiral nature of QH edge modes, such floating contacts induces equal current dividing, one half leaking into the grounding while the other half flowing to the next site. We revise the HN model by adding an energy-dependent dissipation term, $i\gamma(E)=-i\sqrt{8-(E-E_{\mathrm{on}})^2}$ with $E$ being the injecting energy and $E_{\mathrm{on}}=2$ being the on-site energy. The calculated local current shows chirality and nonconservativity in Fig. 5(d). Notably, no matter where the injection point lies and the injecting energy becomes, the local current showcases a consistent decaying ratio, $I_{n+1}=1/2I_n$, ($n>X_0$), which precisely produces the measurement result in Ref. [57].

### VIII. CONCLUSIONS

Our research introduces a transport theory, focusing specifically on the current response, through the reestablishment of the continuity equation for non-Hermitian Hamiltonians within the Schrödinger picture. We contend that the incorporation of anticommutators involving non-Hermitian terms plays a fundamental role, leading to a distinctive revision of the continuity equation that sets it apart from its Hermitian counterparts. Owing to its universal applicability, this approach allows for a robust examination of the inherent nonconservative current phenomena in non-Hermitian systems. Employing the Green's function method, we systematically derive an explicit formula for the local current in both temporal and steady-state cases. The universality of this approach is demonstrated across various dimensional examples, unveiling prominent skin modes, nonreciprocal quantum dots, and corner states. This theoretical framework not only enables a deep investigation into nonconservative current phenomena inherent in non-Hermitian systems but also sets the stage for experimental validation and exploration of non-Hermitian quantum dynamics. The advancements in material growth, device fabrication, and electrical transport measurement techniques highlight the potential of various experimental platforms to validate our theoretical predictions and emphasize the importance of further research into quantum non-Hermitian dynamical evolution. Our research would inspire experimental investigations and contribute to the advancement of non-Hermitian device technology and functionality of non-Hermitian quantum devices.

### ACKNOWLEDGMENTS

This work was financially supported by the National Natural Science Foundation of China (Grants No. 11921005, No. 12374034, and No. 12304052), the Strategic Priority Research Program of Chinese Academy of Sciences (Grant No. XDB28000000), the Innovation Program for Quantum Science and Technology (Grant No. 2021ZD0302400). H.L. is also funded by China Postdoctoral Science Foundation (Grant No. BX20220005).

### APPENDIX A: THE CONTINUITY EQUATION HOLDS REGARDLESS OF BOUNDARY CONDITIONS

Here, we showcase the invariance of the continuity equation regardless of different boundary conditions, open boundary conditions (OBC) and periodic boundary conditions (PBC), emphasizing its universal applicability.

We first discuss on the HN model in Eq. (9) under OBC [52–54] in which case skin modes appear [24,25]. The skin mode $|\phi_n^R\rangle$ satisfies $H|\phi_n^R\rangle = \epsilon_n|\phi_n^R\rangle$, where the wavefunction is $\phi_n^R(x) = \sqrt{2/L}e^{\beta x/(2a)}\sin(n\pi x/L)$ and the eigenenergy is $\epsilon_n = an^2\pi^2/L^2 + \beta^2/4a + i\gamma$ with $L$ being the finite length. For each skin mode, the corresponding $n(x,t)$ exponentially increases or decreases with time $t$ when $\gamma > 0$ or $\gamma < 0$. That is, the particle number $\int_0^L n(x,t)dx$ does not conserve. The nonreciprocal term $\beta$ does not affect the particle number but changes its spatial distribution: the skin mode accumulates at the right or left side with $\beta > 0$ or $\beta < 0$. It is remarkable that such inhomogeneous distribution would not lead to any net current when substituting $\phi_n^R(x)$ into Eq. (3). Here, the continuity equation Eq. (2) holds but simplifies to $\partial_t n(x,t) = (2\gamma/\hbar)n(x,t)$.

Since the conventional bulk-boundary condition no longer holds for the non-Hermitian system [19,21,23], we shall also discuss the HN model under PBC. Here, the eigenstate is in the form of Bloch wave $\phi_k(x) = e^{ikx}$, $k = 2n\pi/L$ and the eigenenergy is $\epsilon_k = ak^2 + ik\beta + i\gamma$. Given one eigenstate $\phi_k$, the density of particle number exponentially varies over time, $\partial_t n = 2(\beta k + \gamma)n$, where both $\gamma$ and $\beta$ play a role. The current density is $j = (2ak/\hbar)n$. When $k \neq 0$, there is a current in the HN ring, the magnitude of which is proportional to the specific wave vector $k$. Such current is evenly distributed in space, $\frac{\partial}{\partial x}j = 0$, meeting with the translational invariance requirement of the PBC. But the current $j$ changes over time, in sync with $n$. As to the continuity equation, the aforementioned intuitive understanding should be revised so that the non-Hermitian terms $\gamma$ and $\beta$ have a direct impact on $n$ and indirect impact on $j$. In a Hermitian system, given a stationary state, both $n$ and $j$ do not change over time. In a non-Hermitian system, $n$ and $j$ vary over time but the relative values ($\frac{n(x_2)}{n(x_1)}$ and $\frac{j(x_2)}{j(x_1)}$) remain constant, that is, $n$ and $j$ synchronously increase or decrease as a whole.

In both boundary conditions, OBC and PBC, the continuity equation Eq. (2) always holds, as stated in Sec. II.

### APPENDIX B: STEADY-STATE CURRENT FORMULA EXPRESSED IN TERMS OF GREEN'S FUNCTION

Below, we derive the steady-state current in details for a time-independent non-Hermitian system. Despite the complex eigenenergies, the non-Hermitian system owning an energy spectrum with nonpositive imaginary parts can also reach a steady state. The (inverse) Fourier transform of Green's functions is defined as follows:

$$G^{r/a}(\epsilon) = \int_{-\infty}^{\infty} G^{r/a}(t,t')e^{i\epsilon(t-t')}dt, \tag{B1}$$

$$G^{r/a}(t,t') = \frac{1}{2\pi}\int_{-\infty}^{\infty} G^{r/a}(\epsilon)e^{-i\epsilon(t-t')}d\epsilon. \tag{B2}$$

Recall that $G^r(t,t') = -i\Theta(t-t')\sum_n e^{-i\epsilon_n(t-t')}|\phi_n^R\rangle\langle\phi_n^L|$ and $G^a(t,t') = i\Theta(t'-t)\sum_n e^{i\epsilon_n^*(t'-t)}|\phi_n^L\rangle\langle\phi_n^R|$. When the imaginary part of any eigenenergy $\epsilon_n$ is nonpositive, both $G^r(\epsilon)$ and $G^a(\epsilon)$ are well defined. Thus, we can derive the steady-state current in the following. When the imaginary part of an eigenenergy $\epsilon_n$ is positive, $G^r(\epsilon)$ and $G^a(\epsilon)$ are ill-defined and the non-Hermitian system may not reach a steady state.

For a non-Hermitian system owning an energy spectrum with nonpositive imaginary parts, we consider a constant injection $|\Phi_0(t')\rangle \equiv |\Phi_0\rangle$ for any time before the observing time, $t' < t$. For any time $t'$, there is a response current at time $t$, $j_\mu(\boldsymbol{r};t,t')$, i.e., Eq. (5) in the main text. Thus, the total local current at $t$ is the sum of all the response with the injection time before $t$. The local current $I_\mu(\boldsymbol{r})$ at position $\boldsymbol{r}$

in the continuous coordinate representation is

$$\begin{aligned} I_\mu(\boldsymbol{r}) &= \int_{-\infty}^{t} dt' \; j_\mu(\boldsymbol{r}; t, t') \\ &= \int_{-\infty}^{t} dt' \, \frac{-2a}{\hbar} \int d\boldsymbol{r}' \int d\boldsymbol{r}'' \mathrm{Im}\left( G^r(\boldsymbol{r}, \boldsymbol{r}''; t, t') \Phi_0(\boldsymbol{r}'') \frac{\partial}{\partial \boldsymbol{r}_\mu} \Phi_0^*(\boldsymbol{r}') G^a(\boldsymbol{r}', \boldsymbol{r}; t', t) \right) \\ &= -\frac{a}{\pi \hbar} \int_{-\infty}^{\infty} d\epsilon \int d\boldsymbol{r}' \int d\boldsymbol{r}'' \, \mathrm{Im}\left( G^r(\boldsymbol{r}, \boldsymbol{r}''; \epsilon) \Phi_0(\boldsymbol{r}'') \Phi_0^*(\boldsymbol{r}') \frac{\partial}{\partial \boldsymbol{r}_\mu} G^a(\boldsymbol{r}', \boldsymbol{r}; \epsilon) \right), \end{aligned} \tag{B3}$$

where $G^{r/a}(\epsilon)$ is inserted and $\frac{1}{2\pi}\int_{-\infty}^{+\infty} dt' e^{-\mathbf{i}(\epsilon-\epsilon')t'} = \delta(\epsilon - \epsilon')$ is used. Such equation shows that the local current at position $\boldsymbol{r}$, $I_\mu(\boldsymbol{r})$ is time independent and reaches the steady state.

Rewrite the steady-state current as $I_\mu(\boldsymbol{r}) = \int_{-\infty}^{+\infty} d\epsilon \;\; j_\mu(\boldsymbol{r}, \epsilon)$. Given an injection with energy $\epsilon$ (here, suppose the injection energy is real), the local current per energy is obtained, $j_\mu(\boldsymbol{r}, \epsilon)$, as shown in Eq. (6).

In the context of lattice models typically used in numerical calculation, the discrete form of the local current can also be obtained using the finite difference method.

Take the expectation value of the local current operator in Eq. (3) with respect to a quantum state at time $t$, $|\Phi(t)\rangle$, and we get

$$\begin{aligned} \langle \hat{\boldsymbol{j}}(\boldsymbol{r}) \rangle_t &= \langle \Phi(t) | \hat{\boldsymbol{j}}(\boldsymbol{r}) | \Phi(t) \rangle \\ &= \frac{a}{i\hbar} (\langle \Phi(t) | \boldsymbol{r} \rangle \nabla \langle \boldsymbol{r} | \Phi(t) \rangle - (\nabla \langle \Phi(t) | \boldsymbol{r} \rangle) \langle \boldsymbol{r} | \Phi(t) \rangle) \\ &= \frac{a}{i\hbar} (\Phi^*(\boldsymbol{r}, t) \nabla \Phi(\boldsymbol{r}, t) - (\nabla \Phi^*(\boldsymbol{r}, t)) \Phi(\boldsymbol{r}, t)). \end{aligned} \tag{B4}$$

Thus, the $\mu$ component of the local current is

$$j_\mu(\boldsymbol{r}, t) = \frac{a}{i\hbar} \left( \Phi^*(\boldsymbol{r}, t) \frac{\partial}{\partial \boldsymbol{r}_\mu} \Phi(\boldsymbol{r}, t) - \left( \frac{\partial}{\partial \boldsymbol{r}_\mu} \Phi^*(\boldsymbol{r}, t) \right) \Phi(\boldsymbol{r}, t) \right). \tag{B5}$$

Denote the local current from lattice $\boldsymbol{R}$ to $\boldsymbol{R} + \boldsymbol{a}_\mu$ as $j(\boldsymbol{R} + \frac{1}{2}\boldsymbol{a}_\mu)$, and it can be discretized as follows:

$$\begin{aligned} j\left(\boldsymbol{R} + \frac{1}{2}\boldsymbol{a}_\mu, t\right) &= \frac{a}{i\hbar} \left( \Phi^*\left(\boldsymbol{R} + \frac{1}{2}\boldsymbol{a}_\mu, t\right) \frac{\partial}{\partial \boldsymbol{r}_\mu} \Phi\left(\boldsymbol{R} + \frac{1}{2}\boldsymbol{a}_\mu, t\right) - \left( \frac{\partial}{\partial \boldsymbol{r}_\mu} \Phi^*\left(\boldsymbol{R} + \frac{1}{2}\boldsymbol{a}_\mu, t\right) \right) \Phi\left(\boldsymbol{R} + \frac{1}{2}\boldsymbol{a}_\mu, t\right) \right) \\ &= \frac{a}{i\hbar} \left( \Phi^*\left(\boldsymbol{R} + \frac{1}{2}\boldsymbol{a}_\mu, t\right) \frac{1}{a_0} [\Phi(\boldsymbol{R} + \boldsymbol{a}_\mu, t) - \Phi(\boldsymbol{R}, t)] - \frac{1}{a_0} [\Phi^*(\boldsymbol{R} + \boldsymbol{a}_\mu, t) - \Phi^*(\boldsymbol{R}, t)] \Phi\left(\boldsymbol{R} + \frac{1}{2}\boldsymbol{a}_\mu, t\right) \right) \\ &= -\frac{2a}{\hbar a_0} \mathrm{Im}(\Phi(\boldsymbol{R}, t) \Phi^*(\boldsymbol{R} + \boldsymbol{a}_\mu, t)). \end{aligned} \tag{B6}$$

Here, $a_0$ is the lattice constant and $\Phi(\boldsymbol{R} + \frac{1}{2}\boldsymbol{a}_\mu, t)$ is substituted by $\frac{1}{2}[\Phi(\boldsymbol{R} + \boldsymbol{a}_\mu, t) + \Phi(\boldsymbol{R}, t)]$.

In terms of the Green's function, the temporal local current as a response to the excitation at time $t'$ is

$$\begin{aligned} j\left(\boldsymbol{R} + \frac{1}{2}\boldsymbol{a}_\mu; t', t\right) &= -\frac{2a}{\hbar a_0} \mathrm{Im}(\langle \boldsymbol{R} | iG^r(t, t') | \Phi_0(t') \rangle \langle \Phi_0(t') | [-iG^a(t', t)] | \boldsymbol{R} + \boldsymbol{a}_\mu \rangle) \\ &= -\frac{2a}{\hbar a_0} \sum_{\boldsymbol{R}'} \sum_{\boldsymbol{R}''} \mathrm{Im}(\langle \boldsymbol{R} | G^r(t, t') | \boldsymbol{R}'' \rangle \langle \boldsymbol{R}'' | \Phi_0(t') \rangle \langle \Phi_0(t') | \boldsymbol{R}' \rangle \langle \boldsymbol{R}' | G^a(t', t) | \boldsymbol{R} + \boldsymbol{a}_\mu \rangle) \\ &= -\frac{2a}{\hbar a_0} \sum_{\boldsymbol{R}'} \sum_{\boldsymbol{R}''} \mathrm{Im}(G^r(\boldsymbol{R}, \boldsymbol{R}''; t, t') \Phi_0(\boldsymbol{R}'', t') \Phi_0^*(\boldsymbol{R}', t') G^a(\boldsymbol{R}', \boldsymbol{R} + \boldsymbol{a}_\mu; t', t)). \end{aligned} \tag{B7}$$

As to the steady state, Eq. (B7) can obtained by the Fourier transformed Green's function denoted as Eq. (B1). Thus, the steady-state local current per energy, $j(\boldsymbol{R} + \frac{1}{2}\boldsymbol{a}_\mu, \epsilon)$, from lattice $\boldsymbol{R}$ to lattice $\boldsymbol{R} + \boldsymbol{a}_\mu$ is obtained as Eq. (7).

## APPENDIX C: CURRENT EXPRESSION REDUCED TO THE TWO-TERMINAL TRANSMISSION COEFFICIENTS FOR THE HERMITIAN CASE

Here, we will show how the local current expression in Eq. (8) ties to the two-terminal transmission coefficient for the Hermitian case.

Suppose a noninteracting Hamiltonian can be separated into two parts $H = H_0 + V$. When $H$ is time independent, the total Green's function in the energy space can also be rewritten as $G(\omega) = \frac{1}{\omega - H}$. For the Hamiltonian $H_0$, the isolated Green's function is $g(\omega) = \frac{1}{\omega - H_0}$. The connection between two Green's function $g(\omega)$ and $G(\omega)$ can be derived as

$$\frac{1}{\omega - H} = \frac{1}{\omega - H_0} + \frac{1}{\omega - H_0} V \frac{1}{\omega - H}.$$

Rewrite the above equation in terms of Green's function and it recovers the Dyson equation,

$$G(\omega) = g(\omega) + g(\omega) V G(\omega). \tag{C1}$$

We assume there is one point-injection at $x_0$. For the comparison with the two-terminal current expression, we consider a semi-infinite chain with the Hamiltonian $H_{\text{semi-inf}} = H_{\text{cen}} + H_{\text{right}} + H_{\text{c}}$. $H_{\text{cen}}$ is the targeted central region where two end points are labeled by $x_{\text{L}}$ and $x_{\text{R}}$. $H_{\text{right}}$ describes a normal lead connected with the central region of which the left end is labeled as $x_{\text{R+1}}$. $H_{\text{c}}$ denotes the coupling, i.e., $H_{\text{c}} = t_{\text{R,R+1}} c^\dagger_{\text{R}} c_{\text{R+1}} + t_{\text{R+1,R}} c^\dagger_{\text{R+1}} c_{\text{R}}$. Then, let $g$ be the Green's function of two isolated regions $H_{\text{cen}}$ and $H_{\text{right}}$ and let $G$ be the Green's function of the whole system $H_{\text{semi-inf}}$. Based on the equation in Eq. (C1), the elements of these two Green's functions are connected by the equation,

$$G^r_{\text{R,L}} = g^r_{\text{R,L}} + g^r_{\text{R,R}} t_{\text{R,R+1}} G^r_{\text{R+1,L}},$$
$$G^r_{\text{R+1,L}} = g^r_{\text{R+1,R+1}} t_{\text{R+1,R}} G^r_{\text{R,L}},$$

where $g^r_{\text{R,R+1}} = g^r_{\text{R+1,R}} = g^r_{\text{R+1,L}} = 0$ is used.

Considering a constant injection at the left end point $x_{\text{L}}$ of the central region, the local current from $x_{\text{R}}$ to $x_{\text{R+1}}$ (i.e., from the center region to the right lead) is $j(\epsilon) = \frac{2}{\hbar}\text{Im}(t_{\text{R,R+1}} G^r_{\text{R+1,L}} \Gamma_{\text{L}} G^a_{\text{L,R}}) = \frac{2}{\hbar}\text{Im}(t_{\text{R,R+1}} g^r_{\text{R+1,R+1}} t_{\text{R+1,R}} G^r_{\text{R,L}} \Gamma_{\text{L}} G^a_{\text{L,R}}) = \frac{2}{\hbar}\text{Im}(\Sigma^r_{\text{R}} G^r_{\text{R,L}} \Gamma_{\text{L}} G^a_{\text{L,R}})$ with the self-energy from the coupling between the center region and the right lead $\Sigma^r_{\text{R}} \equiv t_{\text{R,R+1}} g^r_{\text{R+1,R+1}} t_{\text{R+1,R}}$. Then $j(\epsilon) = \frac{-i}{\hbar}\{\Sigma^r_{\text{R}} G^r_{\text{R,L}} \Gamma_{\text{L}} G^a_{\text{L,R}} - [\Sigma^r_{\text{R}} G^r_{\text{R,L}} \Gamma_{\text{L}} G^a_{\text{L,R}}]^*\} = \frac{-i}{\hbar}\{(\Sigma^r_{\text{R}} - \Sigma^a_{\text{R}}) G^r_{\text{R,L}} \Gamma_{\text{L}} G^a_{\text{L,R}}\} = \frac{1}{\hbar}\Gamma_{\text{R}} G^r_{\text{R,L}} \Gamma_{\text{L}} G^a_{\text{L,R}}$ with $\Gamma_{\text{R}} \equiv -i(\Sigma^r_{\text{R}} - \Sigma^a_{\text{R}})$. Thus, the current from the center region to the right lead exactly corresponds to the two-terminal transmission coefficient.

## APPENDIX D: THE FULFILLMENT OF THE CONTINUITY EQUATION IN CONTINUOUS HN MODEL

Given the continuous HN model in Eq. (9), we will show that the steady-state local current in Eq. (10) satisfies the continuity equation. The retarded and advanced Green's functions defined in Eq. (4) are solved as

$$G^r(x, x_0; \epsilon) = \frac{e^{\frac{1}{2}\frac{\beta}{a}(x-x_0)} e^{i\sqrt{z_p}|x-x_0|}}{2i\sqrt{z_p}},$$

$$G^a(x, x_0; \epsilon) = \frac{e^{-\frac{1}{2}\frac{\beta}{a}(x-x_0)} e^{-\mathbf{i}(\sqrt{z_p})^*|x-x_0|}}{-2i(\sqrt{z_p})^*}.$$

Here, $z_p = |z_p| e^{i\varphi}$ with $|z_p| = \sqrt{(\epsilon/a - \beta^2/4a^2)^2 + (\gamma/a)^2}$, $\tan\varphi = \frac{-\gamma/a}{\epsilon/a - \beta^2/4a^2}$. The particle number at $x$ propagating from the injecting site $x_0$ is

$$n(x, \epsilon) = \frac{1}{2\pi}|A|^2 G^r(x, x_0; \epsilon) G^a(x_0, x; \epsilon) \tag{D1}$$

$$= \frac{1}{2\pi}|A|^2 \frac{1}{4|z_P|} e^{\frac{\beta}{a}(x-x_0)} e^{-2\sqrt{|z_p|}\sin\frac{\varphi}{2}|x-x_0|}. \tag{D2}$$

Note, here, $1/2\pi$ inside $n(x, \epsilon)$ comes from the Fourier transform from time space to energy space.

The local current in Eq. (9) is related to the density of particle number in Eq. (D2) by

$$j(x, \epsilon) = -\frac{2a}{\hbar}(\pm)\sqrt{|z_p|}\cos\frac{\varphi}{2}\, n(x, \epsilon). \tag{D3}$$

Take the derivative of local current $j(x, \epsilon)$, insert Eq. (D3) and we get the continuity equation,

$$\frac{\partial}{\partial x} j(x, \epsilon) = \frac{\beta}{a} j(x, \epsilon) + \frac{2\gamma}{\hbar}\rho(x, \epsilon).$$

The steady-state local current of continuous HN model satisfies the continuity equation, which is exactly the Fourier transform of Eq. (2) under the steady-state condition.

## APPENDIX E: ANALYTICAL LOCAL CURRENT DERIVATION AND THE FULFILLMENT OF THE CONTINUTITY EQUATION IN DISCRETE HN MODEL

Given the discrete HN model in Eq. (11), we will show that the steady-state local current in Eq. (7) satisfies the continuity equation.

In the main text, we calculated the steady-state local current of the HN lattice chain with a continuous pulse-like injection at a certain position $x_0$.

In this Appendix, we comprehensively outline the derivation process for the analytical expression of the local current in an HN lattice model, which proceeds through the following steps: (1) Discretize the continuous Hamiltonian. (2) Derive the surface Green's function for a non-Hermitian semi-infinite lattice. (3) Obtain the analytical expression for the local current. (4) Derive the continuity equation in the lattice framework. (5) Verify the local current's compliance with the continuity equation.

This structured approach allows for a systematic exploration of the analytical derivation of the local current within the HN lattice model.

### 1. Green's function of a semi-infinite non-Hermitian chain

Based on a semi-infinite chain set-up, we can derive the analytical expression for the local current within a lattice model exhibiting non-Hermitian characteristics. In Hermitian systems, many approaches exist for computing the surface

Green's function of a semi-infinite chain. Some methods inherently rely on the boundary condition that necessitates the convergence of the Green's function at an infinite distant point. However, this convergence condition does not always apply to non-Hermitian systems.

To accommodate non-Hermitian systems, where eigenfunctions may not maintain orthonormal relationships, we employ the transfer matrix method to obtain the surface Green's function. We adopt the procedural framework initially introduced in Refs. [58,59] for Hermitian systems.

We divide the translational-invariant lattice chain into principal layers. Within each layer, the degree of freedom is $M$. The principal layers are labeled by ..., $\bar{2}$, $\bar{1}$, 0, 1, 2, ... with the same Hamiltonian $H_{00}$, a $M \times M$ matrix. The hopping between adjacent principal layers is $H_{01}$ and $H_{10}$. For the non-Hermitian model, it is necessary to keep the subscripts of $H_{01}$ and $H_{10}$ since $H_{01}$ is not necessary the Hermitian conjugate of $H_{10}$.

The retarded Green's function of a non-Hermitian chain satisfies $(\epsilon + i\eta - H)G^r = I$. Note that $G^r$ is a function of $\epsilon$ and $\eta$ is a positive infinitesimal. When we focus on the zeroth layer, there comes

$$(\epsilon + i\eta - H_{00})G^r_{00} - H_{01}G^r_{10} - H_{10}G^r_{\bar{1}0} = I_{M\times M}, \tag{E1}$$

where $G^r_{00}$, $G^r_{10}$, and $G^r_{\bar{1}0}$ are the matrix element of $G^r$. And $I_{M\times M}$ is an identity matrix. Also

$$(\epsilon + i\eta - H_{00})G^r_{\bar{n}0} - H_{01}G^r_{\overline{n-1},0} - H_{10}G^r_{\overline{n+1},0} = O_{M\times M}, \tag{E2}$$

$$(\epsilon + i\eta - H_{00})G^r_{n0} - H_{01}G^r_{n+1,0} - H_{10}G^r_{n-1,0} = O_{M\times M}, \tag{E3}$$

with $n = 1, 2, \ldots$. The transfer matrix $T$ is introduced as

$$T = \begin{pmatrix} H_{01}^{-1}(\epsilon + i\eta - H_{00}) & -H_{01}^{-1}H_{10} \\ I_{M\times M} & O_{M\times M} \end{pmatrix}. \tag{E4}$$

By induction, the Green's function meets with the iterative relation

$$\begin{pmatrix} G^r_{n+1,0} \\ G^r_{n,0} \end{pmatrix} = T^n \begin{pmatrix} G^r_{10} \\ G^r_{00} \end{pmatrix}, \quad \begin{pmatrix} G^r_{\bar{n},0} \\ G^r_{\overline{n+1},0} \end{pmatrix} = T^{-n} \begin{pmatrix} G^r_{00} \\ G^r_{\bar{1}0} \end{pmatrix}, \tag{E5}$$

and thus these Green's functions can be expressed in terms of the eigenvector of the transfer matrix $T$. Sort the $2M$ eigenvalues of $T$ to satisfy $|\lambda_1| \leqslant |\lambda_2| \leqslant \ldots |\lambda_M| \leqslant |\lambda_{M+1}| \leqslant \cdots \leqslant |\lambda_{2M}|$, arrange the corresponding eigenvectors into a matrix $\Lambda \equiv (\vec{v_1}, \ldots, \vec{v}_{2M})$ and divide $\Lambda$ into four blocks $\Lambda = \begin{pmatrix} S_2 & S_4 \\ S_1 & S_3 \end{pmatrix}$.

The Green's function of the 0th-layer of a infinite chain is given as

$$G^r_{00} = \left[(\epsilon + i\eta - H_{00}) - H_{01}S_2S_1^{-1} - H_{10}S_3S_4^{-1}\right]^{-1}. \tag{E6}$$

The surface Green's function of the zeroth layer of a left or right semi-infinite chain is obtained by setting either $H_{01} = O_{M\times M}$ or $H_{10} = O_{M\times M}$ in Eq. (E6).

Note that, the upper right block of the transfer matrix defined in Eq. (E4) requires the inverse of $H_{01}$. It can be satisfied either by picking a suitable configuration of principal layers or by introducing the multiplication of several transfer matrices as in [58].

#### 2. Obtain the analytical expression for the local current

For the HN model defined in Eq. (11), we have $H_{00} = \varepsilon_{\rm on} = \frac{2a}{a_0^2} + i\gamma = \varepsilon_0 - i\delta$, $H_{01} = t_{\rm LR}$, $H_{10} = t_{\rm RL}$. Here, $i\gamma$ is replaced by $-i\delta$. For the steady-state transport, $\delta$ is required to be $\delta \geqslant 0$. Substitute them into the transfer matrix defined in Eq. (E3). The eigenvalues are

$$\lambda_\pm(\omega) = \frac{1}{2t_{\rm LR}}\left((\omega + i\delta) \pm \sqrt{(\omega + i\delta)^2 - 4t_{\rm LR}t_{\rm RL}}\right), \tag{E7}$$

where $\omega = \epsilon - \varepsilon_0$ and the relation holds $\lambda_+\lambda_- = \frac{t_{\rm RL}}{t_{\rm LR}}$.

Let $z_q = 4t_{\rm LR}t_{\rm RL} - (\omega + i\delta)^2$. Consider the injection energy range satisfies $\omega^2 < 4t_{\rm LR}t_{\rm RL} + \delta^2$, which means $\mathrm{Re}(z_q) > 0$. Denote $z_q = |z_q|e^{i\varphi}$ and $\sqrt{z_q} = |z_q|e^{i\varphi/2}$. Correspondingly, the two eigenvalues are $\lambda_\pm(\omega) = \frac{1}{2t_{\rm LR}}((\omega + i\delta) \pm i\sqrt{z_q})$, where $\mathrm{Re}(i\sqrt{z_q}) = -\sqrt{|z_q|}\sin\frac{\varphi}{2}$ and $\mathrm{Im}(i\sqrt{z_q}) = \sqrt{|z_q|}\cos\frac{\varphi}{2}$.

The corresponding eigenvectors are $v_\pm = \binom{\lambda_\pm}{1}$. Thus, $\Lambda = \begin{pmatrix} S_2 & S_4 \\ S_1 & S_3 \end{pmatrix} = \begin{pmatrix} \lambda_1 & \lambda_2 \\ 1 & 1 \end{pmatrix}$, where $|\lambda_1| < |\lambda_2|$.

For the left semi-infinite chain, set $H_{01} = t_{\rm LR} = 0$ and substitute into Eq. (E6) so that we obtain the surface Green's function. After some simplification, it becomes $g^r_{\rm sL} = \frac{\lambda_1}{t_{\rm RL}}$. Therefore, the left surface Green's function is

$$\begin{aligned} g^r_{\rm sL}(\epsilon) &= \frac{1}{2t_{\rm LR}t_{\rm RL}}((\omega + i\delta) \pm i\sqrt{z_q}), \\ \mathrm{Re}\big(g^r_{\rm sL}(\epsilon)\big) &= \frac{1}{2t_{\rm LR}t_{\rm RL}}\left(\omega \mp \sqrt{|z_q|}\sin\frac{\varphi}{2}\right), \\ \mathrm{Im}\big(g^r_{\rm sL}(\epsilon)\big) &= \frac{1}{2t_{\rm LR}t_{\rm RL}}\left(\delta \pm \sqrt{|z_q|}\cos\frac{\varphi}{2}\right). \end{aligned} \tag{E8}$$

Since $\lambda_2\lambda_1 = \frac{t_{\rm RL}}{t_{\rm LR}}$, let $|\lambda_2| = \alpha|\lambda_1|$, $\alpha|\lambda_1|^2 = \frac{t_{\rm RL}}{t_{\rm LR}}$. $\alpha = \frac{\omega\ pm\ \sqrt{|z_q|}\sin\frac{\varphi}{2}}{\omega\ mp\ \sqrt{|z_q|}\sin\frac{\varphi}{2}} = -\frac{\delta\ pm\ \sqrt{|z_q|}\cos\frac{\varphi}{2}}{\delta\ mp\ \sqrt{|z_q|}\cos\frac{\varphi}{2}}$, with $pm$ follow the sign of $\lambda_2$.

The local current from site $i$ to site $i+1$ defined in Eq. (8) is

$$j(x_i, \epsilon) = \frac{a}{\hbar a_0^2}2\mathrm{Im}\left[t_{\rm LR}g^r_{\rm sL}\right]\frac{1}{2\pi}|A|^2\left|g^r_{\rm sL}\right|^2\left(\left|t_{\rm LR}g^r_{\rm sL}\right|^2\right)^i, \tag{E9}$$

where $|g^r_{\rm sL}|^2 = |\frac{\lambda_1}{t_{\rm RL}}|^2 = \frac{1}{\alpha t_{\rm RL}^2}\frac{t_{\rm RL}}{t_{\rm LR}} = \frac{1}{t_{\rm RL}t_{\rm LR}}\frac{1}{\alpha}$, $|t_{\rm LR}g^r_{\rm sL}|^2 = \frac{t_{\rm LR}}{t_{\rm RL}}\frac{1}{\alpha}$, and $2\mathrm{Im}[t_{\rm LR}g^r_{\rm sL}] = \frac{1}{t_{\rm RL}}(\delta \pm \sqrt{|z_q|}\cos\frac{\varphi}{2})$.

This is the analytical expression of the steady-state local current of HN lattice model. In the main text, the injection point is set to be $x_0 = 0$ and curves in Fig. 1 with $x < 0$ are plotted according to Eq. (E9). Also, the curves with $x > 0$ can also be derived in a similar procedure by solving a right semi-infinite chain.

#### 3. The continuity equation of a discrete HN lattice model

To derive the explicit form of the continuity equation of the discrete Hamiltonian of a HN model in Eq. (11), we first separate it into three parts, $H = H_0 + H_{\text{anti1}} + H_{\text{anti2}}$,

$$\begin{aligned}
H_0 &= \sum_i \epsilon_0 c_i^\dagger c_i + t^{\text{H}} c_{i+1}^\dagger c_i + t^{\text{H}} c_i^\dagger c_{i+1},\\
H_{\text{anti1}} &= \sum_i t^{\text{A}} c_{i+1}^\dagger c_i - t^{\text{A}} c_i^\dagger c_{i+1},\\
H_{\text{anti2}} &= \sum_i i\gamma c_i^\dagger c_i,
\end{aligned}$$

where $t^{\text{H}} = 1/2(t_{\text{LR}} + t_{\text{RL}})$ and $t^{\text{A}} = 1/2(-t_{\text{LR}} + t_{\text{RL}})$.

Then the time derivative of the particle number at site $i$ is expressed via the (anti)commutation relation, i.e., the concrete form of the continuity equation in Eq. (1),

$$\begin{aligned}
\frac{\partial}{\partial t}\langle \hat{n}_i\rangle_t &= \left\langle \frac{1}{i\hbar}[\hat{n}_i, H_0]\right\rangle_t + \left\langle \frac{1}{i\hbar}\{\hat{n}_i, H_{\text{anti1}}\}\right\rangle_t\\
&\quad + \left\langle \frac{1}{i\hbar}\{\hat{n}_i, H_{\text{anti2}}\}\right\rangle_t.
\end{aligned} \tag{E10}$$

The first commutator reads

$$\begin{aligned}
&\frac{1}{i\hbar}[\hat{n}_i, H_0]\\
&\quad= \frac{1}{i\hbar}[\hat{n}_i, t^{\text{H}} c_i^\dagger c_{i+1} + t^{\text{H}} c_{i+1}^\dagger c_i + t^{\text{H}} c_{i-1}^\dagger c_i + t^{\text{H}} c_i^\dagger c_{i-1}]\\
&\quad= \frac{1}{i\hbar}((t^{\text{H}} c_i^\dagger c_{i+1} - t^{\text{H}} c_{i+1}^\dagger c_i) - (t^{\text{H}} c_{i-1}^\dagger c_i - t^{\text{H}} c_i^\dagger c_{i-1}))\\
&\quad= -\hat{j}(i\to i+1) + \hat{j}(i-1\to i),
\end{aligned}$$

where the local current operator from site $i$ to site $i+1$ and that from site $i-1$ to site $i$ are denoted as

$$\begin{aligned}
\hat{j}(i\to i+1) &= -\frac{1}{i\hbar}(t^{\text{H}} c_i^\dagger c_{i+1} - t^{\text{H}} c_{i+1}^\dagger c_i),\\
\hat{j}(i-1\to i) &= -\frac{1}{i\hbar}(t^{\text{H}} c_{i-1}^\dagger c_i - t^{\text{H}} c_i^\dagger c_{i-1}).
\end{aligned}$$

The first anticommutator reads

$$\begin{aligned}
&\frac{1}{i\hbar}\{\hat{n}_i, H_{\text{anti1}}\}\\
&\quad= \frac{1}{i\hbar}\{\hat{n}_i, -t^{\text{A}} c_i^\dagger c_{i+1} + t^{\text{A}} c_{i+1}^\dagger c_i - t^{\text{A}} c_{i-1}^\dagger c_i + t^{\text{A}} c_i^\dagger c_{i-1}\}\\
&\quad= \frac{1}{i\hbar}(-t^{\text{A}} c_i^\dagger c_{i+1} + t^{\text{A}} c_{i+1}^\dagger c_i) + \frac{1}{i\hbar}(-t^{\text{A}} c_{i-1}^\dagger c_i + t^{\text{A}} c_i^\dagger c_{i-1})\\
&\quad= \frac{t^{\text{A}}}{t^{\text{H}}}\hat{j}(i\to i+1) + \frac{t^{\text{A}}}{t^{\text{H}}}\hat{j}(i-1\to i).
\end{aligned}$$

The second anticommutator term reads

$$\frac{1}{i\hbar}\{\hat{n}_i, H_{\text{anti2}}\} = \frac{1}{i\hbar}\left\{\hat{n}_i, \sum_i i\gamma c_i^\dagger c_i\right\} = \frac{2\gamma}{\hbar}\hat{n}_i.$$

Therefore, the continuity equation in Eq. (E10) becomes

$$\begin{aligned}
\frac{\partial}{\partial t}\langle \hat{n}_i\rangle_t &= -\langle \hat{j}(i\to i+1)\rangle_t + \langle \hat{j}(i-1\to i)\rangle_t\\
&\quad + \frac{t^{\text{A}}}{t^{\text{H}}}\langle \hat{j}(i\to i+1)\rangle_t + \frac{t^{\text{A}}}{t^{\text{H}}}\langle \hat{j}(i-1\to i)\rangle_t\\
&\quad + \frac{2\gamma}{\hbar}\langle \hat{n}_i\rangle_t.
\end{aligned}$$

Redefine that $\frac{\partial}{\partial x}\langle \hat{j}(x=i)\rangle_t = \langle \hat{j}(i\to i+1)\rangle_t - \langle \hat{j}(i-1\to i)\rangle_t$ and $\langle \hat{j}(x=i)\rangle_t = \frac{1}{2}(\langle \hat{j}(i\to i+1)\rangle_t + \langle \hat{j}(i-1\to i)\rangle_t)$. The continuity equation turns to a compact form as follows:

$$\frac{\partial}{\partial t}\langle \hat{n}_i\rangle_t + \frac{\partial}{\partial x}\langle \hat{j}(x=i)\rangle_t = \frac{2t^{\text{A}}}{t^{\text{H}}}\langle \hat{j}(x=i)\rangle_t + \frac{2\gamma}{\hbar}\langle \hat{n}_i\rangle_t, \tag{E11}$$

which is similar to the continuous version.

#### 4. Verify the local current's compliance with the continuity equation

Now check the continuity equation of HN model in the discrete version. Based on the surface Green's function in Eq. (E8) and Dyson equation in Eq. (C1), we can derive the density of particle number at site $i$,

$$\begin{aligned}
n(x_i,\epsilon) &= \frac{1}{2\pi}|A|^2 g_{\text{sL}}^r \left(t_{\text{LR}} g_{\text{sL}}^r\right)^i t_{\text{LR}}^* g_{\text{sL}}^a\\
&= \frac{1}{2\pi}|A|^2 |g_{\text{sL}}^r|^2 \left(\left|t_{\text{LR}} g_{\text{sL}}^r\right|^2\right)^i.
\end{aligned}$$

So we have the relation between $j$ and $n$, i.e., $j(x_i,\epsilon) = \chi\, n(x_i,\epsilon)$, with the coefficient $\chi = -\frac{t^{\text{H}}}{\hbar}2\text{Im}[t_{\text{LR}} g_{\text{sL}}^r]$.

Let abbreviate the variables as $n_i = n(x_i,\epsilon)$, $j_{i\to i+1} = j(x_i,\epsilon)$. Then, the difference of local current at site $i$ is

$$j_{i\to i+1} - j_{i-1\to i} = \chi\left(1 - \left|t_{\text{LR}} g_{\text{sL}}^r\right|^{-2}\right) n_i,$$

and the redefined the local current at site $i$ is

$$j_{i\to i+1} + j_{i-1\to i} = \chi\left(1 + \left|t_{\text{LR}} g_{\text{sL}}^r\right|^{-2}\right) n_i.$$

Label the following expression as $f_l := (j_{i\to i+1} - j_{i-1\to i}) - \frac{2t^{\text{A}}}{t^{\text{H}}}\frac{1}{2}(j_{i\to i+1} + j_{i-1\to i})$, and its explicit form is

$$f_l = \chi\left(1 - \left|t_{\text{LR}} g_{\text{sL}}^r\right|^{-2}\right) n_i - \frac{t^{\text{A}}}{t^{\text{H}}}\chi\left(1 + \left|t_{\text{LR}} g_{\text{sL}}^r\right|^{-2}\right) n_i.$$

By comparing $f_l$ with $n_i$, and employing simplification, we arrive at the relationship $f_l = -\frac{2\delta}{\hbar}n_i$, that is,

$$j_{i\to i+1} - j_{i-1\to i} = \frac{2t^{\text{A}}}{t^{\text{H}}}\frac{1}{2}(j_{i\to i+1} + j_{i-1\to i}) - \frac{2\delta}{\hbar}n_i.$$

Redefine that $\frac{\partial}{\partial x}\langle \hat{j}(x=i)\rangle_\epsilon = \langle \hat{j}(i\to i+1)\rangle_\epsilon - \langle \hat{j}(i-1\to i)\rangle_\epsilon$ and $\langle \hat{j}(x=i)\rangle_\epsilon = \frac{1}{2}(\langle \hat{j}(i\to i+1)\rangle_\epsilon + \langle \hat{j}(i-1\to i)\rangle_\epsilon)$, and replace $-\delta$ by $\gamma$, so the continuity equation turns to a compact form as follows:

$$\frac{\partial}{\partial t}\langle \hat{n}_i\rangle_\epsilon + \frac{\partial}{\partial x}\langle \hat{j}(x=i)\rangle_\epsilon = \frac{2t^{\text{A}}}{t^{\text{H}}}\langle \hat{j}(x=i)\rangle_\epsilon + \frac{2\gamma}{\hbar}\langle \hat{n}_i\rangle_\epsilon.$$

It is the steady-state continuity equation for HN model where the left semi-infinite chain is connected with a source at the rightmost side. As expected, it recovers the Fourier transform of Eq. (E11).


[1] T. Ando, A. B. Fowler, and F. Stern, Electronic properties of two-dimensional systems, Rev. Mod. Phys. **54**, 437 (1982).

[2] W. G. van der Wiel, S. De Franceschi, J. M. Elzerman, T. Fujisawa, S. Tarucha, and L. P. Kouwenhoven, Electron transport through double quantum dots, Rev. Mod. Phys. **75**, 1 (2002).

[3] F. A. Zwanenburg, A. S. Dzurak, A. Morello, M. Y. Simmons, L. C. L. Hollenberg, G. Klimeck, S. Rogge, S. N. Coppersmith, and M. A. Eriksson, Silicon quantum electronics, Rev. Mod. Phys. **85**, 961 (2013).

[4] W. C. Stewart, Current-voltage characteristics of Josephson junctions, Appl. Phys. Lett. **12**, 277 (1968).

[5] T. Fujisawa, T. Hayashi, R. Tomita, and Y. Hirayama, Bidirectional counting of single electrons, Science **312**, 1634 (2006).

[6] K. von Klitzing, G. Dorda, and M. Pepper, New method for high-accuracy determination of the fine-structure constant based on quantized Hall resistance, Phys. Rev. Lett. **45**, 494 (1980).

[7] C.-Z. Chang, J. Zhang, X. Feng, J. Shen, Z. Zhang, M. Guo, K. Li, Y. Ou, P. Wei, L.-L. Wang *et al.*, Experimental observation of the quantum anomalous Hall effect in a magnetic topological insulator, Science **340**, 167 (2013).

[8] Y. J. Deng, Y. J. Yu, M. Z. Shi, Z. X. Guo, Z. H. Xu, J. Wang, X. H. Chen, and Y. B. Zhang, Quantum anomalous Hall effect in intrinsic magnetic topological insulator $MnBi_2Te_4$, Science **367**, 895 (2020).

[9] M. Z. Hasan and C. L. Kane, *Colloquium:* Topological insulators, Rev. Mod. Phys. **82**, 3045 (2010).

[10] X.-L. Qi and S.-C. Zhang, Topological insulators and superconductors, Rev. Mod. Phys. **83**, 1057 (2011).

[11] E. Schrödinger, *Collected papers on Wave Mechanics* (Blackie & Son, London, 1928).

[12] D. J. Griffiths and D. F. Schroeter, *Introduction to Quantum Mechanics*, 3rd ed. (Cambridge University Press, Cambridge, 2018).

[13] D. C. Brody, Biorthogonal quantum mechanics, J. Phys. A: Math. Theor. **47**, 035305 (2014).

[14] A. Ghatak and T. Das, New topological invariants in non-Hermitian systems, J. Phys.: Condens. Matter **31**, 263001 (2019).

[15] Y. Ashida, Z. P. Gong, and M. Ueda, Non-Hermitian physics, Adv. Phys. **69**, 249 (2020).

[16] E. J. Bergholtz, J. C. Budich, and F. K. Kunst, Exceptional topology of non-Hermitian systems, Rev. Mod. Phys. **93**, 015005 (2021).

[17] H. T. Shen, B. Zhen, and L. Fu, Topological band theory for non-Hermitian Hamiltonians, Phys. Rev. Lett. **120**, 146402 (2018).

[18] K. Yokomizo and S. Murakami, Non-Bloch band theory of non-Hermitian systems, Phys. Rev. Lett. **123**, 066404 (2019).

[19] T. E. Lee, Anomalous edge state in a non-Hermitian lattice, Phys. Rev. Lett. **116**, 133903 (2016).

[20] Y. Xiong, Why does bulk boundary correspondence fail in some non-Hermitian topological models, J. Phys. Commun. **2**, 035043 (2018).

[21] F. K. Kunst, E. Edvardsson, J. C. Budich, and E. J. Bergholtz, Biorthogonal bulk-boundary correspondence in non-Hermitian systems, Phys. Rev. Lett. **121**, 026808 (2018).

[22] H. G. Zirnstein, G. Refael, and B. Rosenow, Bulk-boundary correspondence for non-Hermitian Hamiltonians via Green functions, Phys. Rev. Lett. **126**, 216407 (2021).

[23] H. G. Zirnstein and B. Rosenow, Exponentially growing bulk Green functions as signature of nontrivial non-Hermitian winding number in one dimension, Phys. Rev. B **103**, 195157 (2021).

[24] S. Y. Yao, F. Song, and Z. Wang, Non-Hermitian Chern bands, Phys. Rev. Lett. **121**, 136802 (2018).

[25] S. Y. Yao and Z. Wang, Edge states and topological invariants of non-Hermitian systems, Phys. Rev. Lett. **121**, 086803 (2018).

[26] D. S. Borgnia, A. J. Kruchkov, and R.-J. Slager, Non-Hermitian boundary modes and topology, Phys. Rev. Lett. **124**, 056802 (2020).

[27] K. Zhang, Z. S. Yang, and C. Fang, Correspondence between winding numbers and skin modes in non-Hermitian systems, Phys. Rev. Lett. **125**, 126402 (2020).

[28] Y. F. Yi and Z. S. Yang, Non-Hermitian skin modes induced by on-site dissipations and chiral tunneling effect, Phys. Rev. Lett. **125**, 186802 (2020).

[29] J. C. Budich and E. J. Bergholtz, Non-Hermitian topological sensors, Phys. Rev. Lett. **125**, 180403 (2020).

[30] W.-T. Xue, M.-R. Li, Y.-M. Hu, F. Song, and Z. Wang, Simple formulas of directional amplification from non-Bloch band theory, Phys. Rev. B **103**, L241408 (2021).

[31] V. Kornich, Current-voltage characteristics of the normal metal-insulator-PT-symmetric non-Hermitian superconductor junction as a probe of non-Hermitian formalisms, Phys. Rev. Lett. **131**, 116001 (2023).

[32] C. E. Ruter, K. G. Makris, R. El-Ganainy, D. N. Christodoulides, M. Segev, and D. Kip, Observation of parity-time symmetry in optics, Nat. Phys. **6**, 192 (2010).

[33] S. Weimann, M. Kremer, Y. Plotnik, Y. Lumer, S. Nolte, K. G. Makris, M. Segev, M. Rechtsman, and C. A. Szameit, Topologically protected bound states in photonic parity-time-symmetric crystals, Nat. Mater. **16**, 433 (2017).

[34] S. K. Ozdemir, S. Rotter, F. Nori, and L. Yang, Parity-time symmetry and exceptional points in photonics, Nat. Mater. **18**, 783 (2019).

[35] C. H. Lee, S. Imhof, C. Berger, F. Bayer, J. Brehm, L. W. Molenkamp, T. Kiessling, and R. Thomale, Topolectrical circuits, Commun. Phys. **1**, 39 (2018).

[36] T. Helbig, T. Hofmann, S. Imhof, M. Abdelghany, T. Kiessling, L. W. Molenkamp, C. H. Lee, A. Szameit, M. Greiter, and R. Thomale, Generalized bulk-boundary correspondence in non-Hermitian topolectrical circuits, Nat. Phys. **16**, 747 (2020).

[37] A. Ghatak, M. Brandenbourger, J. van Wezel, and C. Coulais, Observation of non-Hermitian topology and its bulk-edge correspondence in an active mechanical metamaterial, Proc. Natl. Acad. Sci. USA **117**, 29561 (2020).

[38] J. M. Li, A. K. Harterg, J. Liu, L. de Melo, Y. N. Joglekar, and L. Luo, Observation of parity-time symmetry breaking

transitions in a dissipative Floquet system of ultracold atoms, Nat. Commun. **10**, 855 (2019).

[39] L. Xiao, T. S. Deng, K. K. Wang, G. Y. Zhu, Z. Wang, W. Yi, and P. Xue, Non-Hermitian bulk-boundary correspondence in quantum dynamics, Nat. Phys. **16**, 761 (2020).

[40] D. Sticlet, B. Dóra, and C. P. Moca, Kubo formula for non-Hermitian systems and tachyon optical conductivity, Phys. Rev. Lett. **128**, 016802 (2022).

[41] A. J. Daley, Quantum trajectories and open many-body quantum systems, Adv. Phys. **63**, 77 (2014).

[42] G. Barontini, R. Labouvie, F. Stubenrauch, A. Vogler, V. Guarrera, and H. Ott, Controlling the dynamics of an open many-body quantum system with localized dissipation, Phys. Rev. Lett. **110**, 035302 (2013).

[43] Y. Meir and N. S. Wingreen, Landauer formula for the current through an interacting electron region, Phys. Rev. Lett. **68**, 2512 (1992).

[44] A.-P. Jauho, N. S. Wingreen, and Y. Meir, Time-dependent transport in interacting and noninteracting resonant-tunneling systems, Phys. Rev. B **50**, 5528 (1994).

[45] H. Haug and A.-P. Jauho, *Quantum Kinetics in Transport and Optics of Semiconductors* (Springer, New York, 2008), Vol. 2.

[46] Q.-F. Sun and X. C. Xie, Heat generation by electric current in mesoscopic devices, Phys. Rev. B **75**, 155306 (2007).

[47] J.-S. Wang, J. Wang, and J. T. Lü, Quantum thermal transport in nanostructures, Eur. Phys. J. B **62**, 381 (2008).

[48] C. Caroli, R. Combescot, P. Nozieres, and D. Saint-James, Direct calculation of the tunneling current, J. Phys. C: Solid State Phys. **4**, 916 (1971).

[49] C. Caroli, R. Combescot, D. Lederer, P. Nozieres, and D. Saint-James, A direct calculation of the tunnelling current. II. Free electron description, J. Phys. C: Solid State Phys. **4**, 2598 (1971).

[50] E. N. Economou, *Green's Functions in Quantum Physics* (Springer, Berlin, Heidelberg, 2006), Vol. 3.

[51] H. Jiang, L. Wang, Q.-F. Sun, and X. C. Xie, Numerical study of the topological Anderson insulator in HgTe/CdTe quantum wells, Phys. Rev. B **80**, 165316 (2009).

[52] N. Hatano and D. R. Nelson, Localization transitions in non-Hermitian quantum mechanics, Phys. Rev. Lett. **77**, 570 (1996).

[53] N. Hatano and D. R. Nelson, Vortex pinning and non-Hermitian quantum mechanics, Phys. Rev. B **56**, 8651 (1997).

[54] N. Hatano and D. R. Nelson, Non-Hermitian delocalization and eigenfunctions, Phys. Rev. B **58**, 8384 (1998).

[55] L. L. Chang, L. Esaki, and R. Tsu, Resonant tunneling in semiconductor double barriers, Appl. Phys. Lett. **24**, 593 (1974).

[56] K. Zhang, Z. Yang, and C. Fang, Universal non-Hermitian skin effect in two and higher dimensions, Nat. Commun. **13**, 2496 (2022).

[57] K. Ochkan, R. Chaturvedi, V. Könye, L. Veyrat, R. Giraud, D. Mailly, A. Cavanna, U. Gennser, E. M. Hankiewicz, B. Büchner *et al.*, Non-hermitian topology in a multi-terminal quantum Hall device, Nat. Phys. **20**, 395 (2024).

[58] D. H. Lee and J. D. Joannopoulos, Simple scheme for surface-band calculations. I, Phys. Rev. B **23**, 4988 (1981).

[59] D. H. Lee and J. D. Joannopoulos, Simple scheme for surface-band calculations. II. The Green's function, Phys. Rev. B **23**, 4997 (1981).